ISSN 1516-392X

ISOTROPIC AND KINEMATIC HARDENING MODELS FOR NON-PROPORTIONAL MULTIAXIAL LOADING HISTORIES[1]

Marco Antonio Meggiolaro[2]
Jaime Tupiassú Pinho de Castro[3]

Abstract
It is well known that the uniaxial Ramberg-Osgood model cannot be used to correlate principal stresses and strains under multiaxial loading. But, to calculate multiaxial fatigue damage, it is frequently necessary to obtain the multiaxial stresses from measured elastic-plastic strains. To tackle this task, an efficient model is proposed to obtain the multiaxial stress-strain history in the non-proportional case, considering both isotropic and kinematic hardening. An improved version of the Mròz multi-yield surface model is used to calculate the Bauschinger effect under multiaxial loading in the deviatoric stress space, allowing the yield surface to translate with no change in its size or shape, following Garud's hypothesis. Moreover, an algorithm is presented to obtain the multiaxial hysteresis loops, including the effects of isotropic and kinematic hardening due to cyclic loads.
Key words: Multiaxial fatigue; Non-proportional loading; Isotropic and kinematic hardening; Incremental plasticity; Multi-yield-surface algorithm.

MODELOS DE ENCRUAMENTO ISOTRÓPICO E CINEMÁTICO PARA HISTÓRIAS DE CARREGAMENTO MULTIAXIAL NÃO-PROPORCIONAL

Resumo
O modelo uniaxial de Ramberg-Osgood não pode ser usado para correlacionar tensões e deformações principais sob cargas multiaxiais. Mas para calcular o dano multiaxial à fadiga é frequentemente necessário obter as tensões multiaxiais a partir de deformações elastoplásticas medidas. Para cumprir esta tarefa, um modelo eficiente é proposto para obter a história de tensão-deformação no caso não-proporcional, considerando ambos os encruamentos isotrópico e cinemático. Uma versão melhorada do modelo de múltiplas superfícies de escoamento de Mròz é usado para calcular o efeito de Bauschinger sob cargas multiaxiais no espaço de tensões desviatórias, permitindo que a superfície de escoamento translade sem mudar seu tamanho ou forma, segundo a hipótese de Garud. Além disso, um algoritmo é apresentado para obter os laços de histerese multiaxiais, incluindo efeitos de encruamento isotrópico e cinemático.
Palavras chave: Fadiga multiaxial; Carregamento não-proporcional; Encruamento isotrópico e cinemático; Plasticidade incremental; Algoritmo de múltiplas superfícies de escoamento.

[1] *Technical contribution to 65th ABM Annual Congress, July, 26th to 30h, 2010, Rio de Janeiro, RJ, Brazil.*
[2] *Engenheiro Mecânico, Ph.D., Professor Dept. Eng. Mecânica, PUC-Rio*

1 INTRODUÇÃO

In most engineering applications, either the stress or the strain history is known, but not both. When designing a new component, it is common to calculate or estimate the stress history from measured or specified design loads, whereas in most structural integrity evaluations (of an existing component) only the strain history can be measured using strain gage rosettes, for example. But the best multiaxial fatigue damage models require the knowledge of both the stress and the corresponding strain histories to quantify the consequent damage parameter.[1-3]
For linear elastic histories, it is trivial to correlate the stresses with the strains using Hooke's law. For elastoplastic proportional histories, where the principal directions remain fixed, this can be done using the (total) stress-strain models from the previous section. But to properly reproduce the stress-strain hysteresis loops in NP elastoplastic histories, which depend on the load path, it is necessary to use incremental plasticity models to correlate infinitesimal changes in all stress components with the associated strain components, and vice-versa. They are based on 3 equations: the yield function, which describes combinations of stresses that lead to plastic flow; the flow rule, which describes the relationship between stresses and plastic strains; and the hardening rule, which defines how the yield criterion changes with plastic straining. These equations are discussed and applied in the following sections.

2 STRESS AND STRAIN TENSORS

A convenient way to represent the equations in incremental plasticity is to represent stress and strain tensors as 9-dimensional column vectors:

$$\bar{\sigma} = \left[\sigma_x \quad \sigma_y \quad \sigma_z \quad \tau_{xy} \quad \tau_{yx} \quad \tau_{xz} \quad \tau_{zx} \quad \tau_{yz} \quad \tau_{zy}\right]^T$$

$$\bar{\varepsilon} = \left[\varepsilon_x \quad \varepsilon_y \quad \varepsilon_z \quad \varepsilon_{xy} \quad \varepsilon_{yx} \quad \varepsilon_{xz} \quad \varepsilon_{zx} \quad \varepsilon_{yz} \quad \varepsilon_{zy}\right]^T$$

where $\tau_{ij} = \tau_{ji}$ (or $\tau_{xy} = \tau_{yx}$, $\tau_{xz} = \tau_{zx}$, $\tau_{yz} = \tau_{zy}$), $\varepsilon_{ij} = \varepsilon_{ji}$, $\gamma_{ij} = 2\varepsilon_{ij}$ (meaning $\gamma_{xy} = \varepsilon_{xy} + \varepsilon_{yx} = 2\varepsilon_{xy}$, etc.), and **T** stands for the transpose of a vector. The elastoplastic strain $\bar{\varepsilon}$ is the sum of the elastic and plastic components $\bar{\varepsilon} = \bar{\varepsilon}_e + \bar{\varepsilon}_p$, where

$$\bar{\varepsilon}_e = \left[\varepsilon_{x_e} \quad \varepsilon_{y_e} \quad \varepsilon_{z_e} \quad \varepsilon_{xy_e} \quad \varepsilon_{yx_e} \quad \varepsilon_{xz_e} \quad \varepsilon_{zx_e} \quad \varepsilon_{yz_e} \quad \varepsilon_{zy_e}\right]^T$$

$$\bar{\varepsilon}_p = \left[\varepsilon_{x_p} \quad \varepsilon_{y_p} \quad \varepsilon_{z_p} \quad \varepsilon_{xy_p} \quad \varepsilon_{yx_p} \quad \varepsilon_{xz_p} \quad \varepsilon_{zx_p} \quad \varepsilon_{yz_p} \quad \varepsilon_{zy_p}\right]^T$$

Hooke's law can then be expressed in vectorial form by $\bar{\varepsilon}_e = \bar{E}^{-1} \cdot \bar{\sigma}$, where $\bar{E}^{-1}$ is Hooke's elastic compliance matrix, the inverse of the stiffness matrix. It is also convenient to define the hidrostatic stress and strain vectors

$$\bar{\sigma}_h = \sigma_h \cdot \left[1 \quad 1 \quad 1 \quad 0 \quad 0 \quad 0 \quad 0 \quad 0 \quad 0\right]^T$$

$$\bar{\varepsilon}_h = \varepsilon_h \cdot \left[1 \quad 1 \quad 1 \quad 0 \quad 0 \quad 0 \quad 0 \quad 0 \quad 0\right]^T$$

where $\sigma_h = (\sigma_x + \sigma_y + \sigma_z)/3$ and $\varepsilon_h = (\varepsilon_x + \varepsilon_y + \varepsilon_z)/3$.

3 YIELD FUNCTION AND FLOW RULE

The yield function is an equation in the stress space $\bar{\sigma}$ that describes the combinations of stress components which cause yielding. The most used yield function is based on the Mises yield criterion[1]

$$F = \sigma_x^2 + \sigma_y^2 + \sigma_z^2 - \sigma_x\sigma_y - \sigma_x\sigma_z - \sigma_y\sigma_z + 3\cdot\left(\tau_{xy}^2 + \tau_{yz}^2 + \tau_{zx}^2\right) - S_Y^2 = 0$$

where S_Y is the yield strength (either monotonic or cyclic, or some value in between, depending on the application). This yield function assumes that the material is isotropic, since the subscripts x, y and z can be interchanged without changing the equation. It also assumes that the material is pressure-insensitive, because it is independent of the hydrostatic stress σ_h. Geometrically, the Mises yield function **F = 0** describes the surface of a hyperellipsoid in the 9-dimensional stress space. When represented in 2D in a σ_x-σ_y diagram, it results in the boundary of an ellipsis rotated 45° from the x axis, see the left figure in Figure 1.

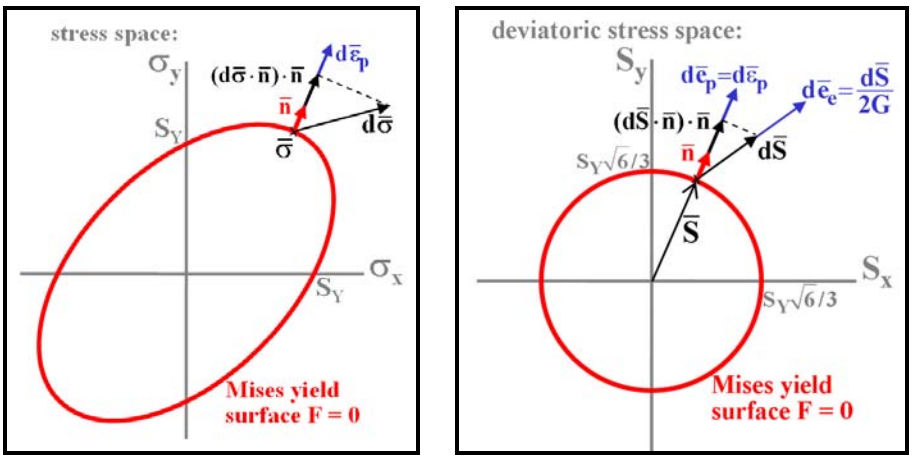

Figure 1. Mises yield surface in the σ_x-σ_y stress space (left) and in the S_x-S_y stress space (right), showing a normal vector and the flow rule.

If at some stress state $\bar{\sigma}$ the yield function $F(\bar{\sigma}, S_Y) < 0$, then $\bar{\sigma}$ is inside the yield surface, and any infinitesimal stress variation $d\bar{\sigma}$ will lead to a purely elastic strain variation $d\bar{\varepsilon} = d\bar{\varepsilon}_e = \bar{\bar{E}}^{-1}\cdot d\bar{\sigma}$, since $d\bar{\varepsilon}_p = 0$. But if $\bar{\sigma}$ is on the yield surface and its variation $d\bar{\sigma}$ is in the outward direction of **F = 0** (i.e. **dF > 0**), then the material will yield and generate a plastic strain increment given by the Prandtl-Reuss flow rule

$$d\bar{\varepsilon}_p = \frac{1}{C}\cdot(d\bar{\sigma}\cdot\bar{n})\cdot\bar{n}$$

where **C** is called the generalized plastic modulus, and $\bar{n}$ is the normal unit vector perpendicular to the surface **F = 0** at the current state $\bar{\sigma}$, given by

$$\bar{n} = \frac{\partial F/\partial\bar{\sigma}}{|\partial F/\partial\bar{\sigma}|}$$

where $|\partial F/\partial\bar{\sigma}|$ stands for the norm of the gradient

$$\frac{\partial F}{\partial\bar{\sigma}} = \left[\frac{\partial F}{\partial\sigma_x}\ \frac{\partial F}{\partial\sigma_y}\ \frac{\partial F}{\partial\sigma_z}\ \frac{\partial F}{\partial\tau_{xy}}\ \frac{\partial F}{\partial\tau_{yx}}\ \frac{\partial F}{\partial\tau_{xz}}\ \frac{\partial F}{\partial\tau_{zx}}\ \frac{\partial F}{\partial\tau_{yz}}\ \frac{\partial F}{\partial\tau_{zy}}\right]^T$$

ISSN 1516-392X

Note also that the flow rule is only valid if $d\bar{\sigma}\cdot\bar{n}$ is not negative, otherwise $\bar{\sigma}$ would be moving in stress space in the inward direction of the yield surface. From the Mises yield function, it is found that

$$\frac{\partial F}{\partial \bar{\sigma}} = \left[2\sigma_x - \sigma_y - \sigma_z \quad 2\sigma_y - \sigma_x - \sigma_z \quad 2\sigma_z - \sigma_x - \sigma_y \quad 3\tau_{xy} \quad 3\tau_{yx} \quad 3\tau_{xz} \quad 3\tau_{zx} \quad 3\tau_{yz} \quad 3\tau_{zy}\right]^T$$

The generalized plastic modulus **C** can then be obtained from the uniaxial case using the Ramberg-Osgood equation, assuming $\bar{\sigma} = \left[\sigma_x \quad 0 \quad 0 \quad 0 \quad 0 \quad 0 \quad 0 \quad 0 \quad 0\right]^T$. The gradient $\partial F/\partial\bar{\sigma}$ in this case becomes

$$\frac{\partial F}{\partial \bar{\sigma}} = \left[2\sigma_x \quad -\sigma_x \quad -\sigma_x \quad 0 \quad 0 \quad 0 \quad 0 \quad 0 \quad 0\right]^T$$

where $|\partial F/\partial\bar{\sigma}| = \sigma_x\sqrt{6}$. A variation $d\bar{\sigma} = \left[d\sigma_x \quad 0 \quad 0 \quad 0 \quad 0 \quad 0 \quad 0 \quad 0 \quad 0\right]^T$ in the outward direction of the yield surface will cause then a plastic strain variation

$$d\bar{\varepsilon}_p = \frac{1}{C}\cdot\frac{(d\bar{\sigma}\cdot\partial F/\partial\bar{\sigma})\cdot\partial F/\partial\bar{\sigma}}{|\partial F/\partial\bar{\sigma}|^2} = \frac{1}{C}\cdot\frac{2\sigma_x d\sigma_x}{6\sigma_x^2}\cdot\left[2\sigma_x \quad -\sigma_x \quad -\sigma_x \quad 0 \quad 0 \quad 0 \quad 0 \quad 0 \quad 0\right]^T$$

therefore its **x** component is $d\varepsilon_{xp} = 2\cdot d\sigma_x/3C \Rightarrow C = 2\cdot d\sigma_x/3d\varepsilon_{xp}$. On the other hand, from the cyclic Ramberg-Osgood equation

$$\varepsilon_{xp} = \left(\frac{\sigma_x}{H_c}\right)^{1/h_c} \Rightarrow d\varepsilon_{xp} = \frac{1}{h_c}\cdot\left(\frac{\sigma_x}{H_c}\right)^{1/h_c - 1}\cdot\frac{d\sigma_x}{H_c} = \frac{2\,d\sigma_x}{3C} \Rightarrow C = \frac{2}{3}\cdot h_c H_c\left(\frac{\sigma_x}{H_c}\right)^{1-1/h_c}$$

4 DEVIATORIC STRESS AND STRAIN TENSORS

It is much simpler to represent the Mises yield function, the Prandtl-Reuss flow rule and Hooke's law with respect to the deviatoric stress and strain tensors $\bar{S}$ and $\bar{e}$, instead of $\bar{\sigma}$ and $\bar{\varepsilon}$, obtained from the difference between the stress or strain tensors and their hydrostatic component

$$\bar{S} = \bar{\sigma} - \bar{\sigma}_h = \left[S_x \quad S_y \quad S_z \quad \tau_{xy} \quad \tau_{yx} \quad \tau_{xz} \quad \tau_{zx} \quad \tau_{yz} \quad \tau_{zy}\right]^T$$

$$\bar{e} = \bar{\varepsilon} - \bar{\varepsilon}_h = \left[e_x \quad e_y \quad e_z \quad \varepsilon_{xy} \quad \varepsilon_{yx} \quad \varepsilon_{xz} \quad \varepsilon_{zx} \quad \varepsilon_{yz} \quad \varepsilon_{zy}\right]^T$$

where $S_x = \sigma_x - \sigma_h = (2\sigma_x - \sigma_y - \sigma_z)/3$, $S_y = (2\sigma_y - \sigma_x - \sigma_z)/3$, $S_z = (2\sigma_z - \sigma_x - \sigma_y)/3$, and $e_x = \varepsilon_x - \varepsilon_h = (2\varepsilon_x - \varepsilon_y - \varepsilon_z)/3$, $e_y = (2\varepsilon_y - \varepsilon_x - \varepsilon_z)/3$, $e_z = (2\varepsilon_z - \varepsilon_x - \varepsilon_y)/3$. The deviatoric stress points (S_x, S_y, S_z) describe a plane in the (σ_x, σ_y, σ_z) space called deviatoric plane or π-plane. Note that $S_x + S_y + S_z = (\sigma_x + \sigma_y + \sigma_z) - 3\sigma_h = 0$ and $e_x + e_y + e_z = (\varepsilon_x + \varepsilon_y + \varepsilon_z) - 3\varepsilon_h = 0$.

The deviatoric strain can be represented as the sum of its elastic and plastic components

$$\bar{e}_e = \left[e_{xe} \quad e_{ye} \quad e_{ze} \quad \varepsilon_{xye} \quad \varepsilon_{yxe} \quad \varepsilon_{xze} \quad \varepsilon_{zxe} \quad \varepsilon_{yze} \quad \varepsilon_{zye}\right]^T$$

$$\bar{e}_p = \left[e_{xp} \quad e_{yp} \quad e_{zp} \quad \varepsilon_{xyp} \quad \varepsilon_{yxp} \quad \varepsilon_{xzp} \quad \varepsilon_{zxp} \quad \varepsilon_{yzp} \quad \varepsilon_{zyp}\right]^T$$

In the deviatoric space, it follows that Hooke's law simply becomes $\bar{e}_e = \bar{S}/2G$, where $G = E/[2\cdot(1+\nu)]$. Therefore, since the elastic component of the deviatoric strain is always parallel to the deviatoric stress, they're related by the scalar **2G**, without the

need to use Hooke's 9×9 elastic compliance matrix, simplifying the calculations. The incremental deviatoric stresses and elastic strains are related by $d\bar{e}_e = d\bar{S}/2G$.

As the Mises yield function is pressure-insensitive, the hidrostatic stresses cannot cause plastic strains, therefore these components are always elastic and correlated by Hooke's law $\varepsilon_h = \sigma_h / 3K$, where $K = E/[3(1-2\nu)]$ is the bulk modulus of the material, which measures its resistance to uniform compression. Therefore, $\bar{\varepsilon}_h = \bar{\sigma}_h/3K$ and $d\bar{\varepsilon}_h = d\bar{\sigma}_h/3K$.

It follows that the increment $d\bar{e} = d\bar{e}_e + d\bar{e}_p = (d\bar{\varepsilon}_e - d\bar{\varepsilon}_h) + d\bar{\varepsilon}_p$. Since the hydrostatic component $\bar{\varepsilon}_h$ is elastic, the correspondence between elastic and plastic strain increments results in $d\bar{e}_e = d\bar{\varepsilon}_e - d\bar{\varepsilon}_h$ and $d\bar{e}_p = d\bar{\varepsilon}_p$. Another advantage of using the deviatoric space is that the Mises yield function simply becomes

$$F = \frac{3}{2}\cdot\left[S_x^2 + S_y^2 + S_z^2 + \tau_{xy}^2 + \tau_{yx}^2 + \tau_{xz}^2 + \tau_{zx}^2 + \tau_{yz}^2 + \tau_{zy}^2\right] - S_Y^2 = \frac{3}{2}\cdot\left\{|\bar{S}|^2 - \left(S_Y\sqrt{6}/3\right)^2\right\} = 0$$

where $|\bar{S}|$ is the norm of the deviatoric stress tensor. So, from the above equation the Mises yield surface is simply a 9-dimensional sphere (a hypersphere) with radius $S_Y\sqrt{6}/3$ in the deviatoric space. When represented in 2D in an S_x-S_y diagram, it results in the boundary of a circle, see the right figure in Fig. 1. The use of hyperspheres, instead of hyperellipsoids, greatly simplifies the incremental plasticity algorithms, especially when the hardening rules are introduced, in the next section.

It is possible to show that the normal unit vector $\bar{n}$ perpendicular to the surface $F = 0$ at the current state $\bar{S}$ has the same expression as in the stress space

$$\bar{n} = \frac{\partial F/\partial \bar{S}}{|\partial F/\partial \bar{S}|} = \frac{\partial F/\partial \bar{\sigma}}{|\partial F/\partial \bar{\sigma}|}$$

From $d\bar{e}_p = d\bar{\varepsilon}_p$ and $d\bar{S}\cdot\bar{n} = d\bar{\sigma}\cdot\bar{n}$, the Prandtl-Reuss flow rule results in

$$d\bar{\varepsilon}_p = \frac{1}{C}\cdot(d\bar{\sigma}\cdot\bar{n})\cdot\bar{n} \quad \Rightarrow \quad d\bar{e}_p = \frac{1}{C}\cdot(d\bar{S}\cdot\bar{n})\cdot\bar{n}$$

4.1 Direct Problem (Given the Stress History)

If $\bar{\sigma}$ is on the yield surface and its variation $d\bar{\sigma}$ is in the outward direction of $F = 0$, then the above equations are enough to calculate the strain increment $d\bar{\varepsilon}$ as a function of $\bar{\sigma}$ and $d\bar{\sigma}$ from a given stress history from the hydrostatic stresses

$$\begin{cases} \bar{\sigma} \;\Rightarrow\; \sigma_h = (\sigma_x + \sigma_y + \sigma_z)/3 \;\Rightarrow\; \bar{\sigma}_h = \sigma_h\cdot[1\ \ 1\ \ 1\ \ 0\ \ 0\ \ 0\ \ 0\ \ 0\ \ 0]^T \\ d\bar{\sigma} \;\Rightarrow\; d\sigma_h = (d\sigma_x + d\sigma_y + d\sigma_z)/3 \;\Rightarrow\; d\bar{\sigma}_h = d\sigma_h\cdot[1\ \ 1\ \ 1\ \ 0\ \ 0\ \ 0\ \ 0\ \ 0\ \ 0]^T \end{cases}$$

followed by the calculation of the deviatoric strain increment $d\bar{e}$ from the current C and $\bar{n}$ and its conversion to $d\bar{\varepsilon}$ using

$$\left.\begin{array}{l} \bar{S} = \bar{\sigma} - \bar{\sigma}_h \\ d\bar{S} = d\bar{\sigma} - d\bar{\sigma}_h \end{array}\right\} \Rightarrow d\bar{e} = \frac{d\bar{S}}{2G} + \frac{1}{C}\cdot(d\bar{S}\cdot\bar{n})\cdot\bar{n} \;\Rightarrow\; d\bar{\varepsilon} = d\bar{e} + d\bar{\varepsilon}_h = d\bar{e} + \frac{d\bar{\sigma}_h}{3K}$$

The above formulation is valid for a general 3D stress history. But in most practical design problems, the stress history is given on a free surface (assumed perpendicular to the z direction) through the components $\{\sigma_x, \sigma_y, \tau_{xy}\}$ and their

variations $\{d\sigma_x, d\sigma_y, d\tau_{xy}\}$. Since $\sigma_z = \tau_{xz} = \tau_{zx} = \tau_{yz} = \tau_{zy} = 0$ and $\tau_{yx} = \tau_{xy}$, the stress tensors used in this case are

$$\begin{cases} \bar{\sigma} = \left[\sigma_x \quad \sigma_y \quad 0 \quad \tau_{xy} \quad \tau_{xy} \quad 0 \quad 0 \quad 0 \quad 0\right]^T \\ d\bar{\sigma} = \left[d\sigma_x \quad d\sigma_y \quad 0 \quad d\tau_{xy} \quad d\tau_{xy} \quad 0 \quad 0 \quad 0 \quad 0\right]^T \end{cases}$$

and the resulting strain increment should only have the components

$$d\bar{\varepsilon} = \left[d\varepsilon_x \quad d\varepsilon_y \quad d\varepsilon_z \quad d\varepsilon_{xy} \quad d\varepsilon_{yx} \quad 0 \quad 0 \quad 0 \quad 0\right]^T$$

where $d\gamma_{xy} = d\varepsilon_{xy} + d\varepsilon_{yx} = 2d\varepsilon_{xy}$, and the strain variation $d\varepsilon_z$ is usually non-zero due to the Poisson effect.

Inverse problem (given the strain history)

The inverse problem of calculating $d\bar{\sigma}$ as a function of $\bar{\varepsilon}$ and $d\bar{\varepsilon}$, necessary if the strain history is given, requires the following derivations

$$d\bar{e} = \frac{d\bar{S}}{2G} + \frac{1}{C}\cdot(d\bar{S}\cdot\bar{n})\cdot\bar{n} \;\Rightarrow\; d\bar{e}\cdot\bar{n} = \frac{d\bar{S}\cdot\bar{n}}{2G} + \frac{1}{C}\cdot(d\bar{S}\cdot\bar{n})\cdot\bar{n}\cdot\bar{n} \;\Rightarrow$$

$$\Rightarrow\; (d\bar{\varepsilon} - d\bar{\varepsilon}_h)\cdot\bar{n} = d\bar{\varepsilon}\cdot\bar{n} = \left(\frac{1}{2G} + \frac{1}{C}\right)\cdot d\bar{S}\cdot\bar{n} \;\Rightarrow\; d\bar{S}\cdot\bar{n} = \frac{2GC}{2G+C}d\bar{\varepsilon}\cdot\bar{n}$$

which, combined with the Prandtl-Reuss flow rule gives

$$d\bar{\varepsilon}_p = d\bar{e}_p = \frac{1}{C}\cdot(d\bar{S}\cdot\bar{n})\cdot\bar{n} = \frac{2G}{2G+C}\cdot(d\bar{\varepsilon}\cdot\bar{n})\cdot\bar{n}$$

So, if $\bar{\varepsilon}$ and $d\bar{\varepsilon}$ are given and it is known that $\bar{\sigma}$ is on the yield surface, and assuming that the unknown variation $d\bar{\sigma}$ is in the outward direction of $\mathbf{F = 0}$, then such $d\bar{\sigma}$ can be calculated by computing the hydrostatic strains

$$\begin{cases} \bar{\varepsilon} \;\Rightarrow\; \varepsilon_h = (\varepsilon_x + \varepsilon_y + \varepsilon_z)/3 \;\Rightarrow\; \bar{\varepsilon}_h = \varepsilon_h\cdot\left[1 \quad 1 \quad 1 \quad 0 \quad 0 \quad 0 \quad 0 \quad 0 \quad 0\right]^T \\ d\bar{\varepsilon} \;\Rightarrow\; d\varepsilon_h = (d\varepsilon_x + d\varepsilon_y + d\varepsilon_z)/3 \;\Rightarrow\; d\bar{\varepsilon}_h = d\varepsilon_h\cdot\left[1 \quad 1 \quad 1 \quad 0 \quad 0 \quad 0 \quad 0 \quad 0 \quad 0\right]^T \end{cases}$$

followed by the calculation of the deviatoric stress increment $d\bar{S}$ from the current $\mathbf{C}$ and $\bar{n}$

$$d\bar{S} = 2G\cdot d\bar{e}_e = 2G\cdot[d\bar{\varepsilon} - d\bar{\varepsilon}_h - d\bar{\varepsilon}_p] = 2G\cdot[d\bar{\varepsilon} - d\bar{\varepsilon}_h - \frac{2G}{2G+C}\cdot(d\bar{\varepsilon}\cdot\bar{n})\cdot\bar{n}]$$

and its conversion to $d\bar{\sigma}$ using

$$d\bar{\sigma} = d\bar{S} + d\bar{\sigma}_h = d\bar{S} + 3K\cdot d\bar{\varepsilon}_h$$

Note that the above equation is only valid if the resulting $d\bar{\sigma}$ is in the outward direction of the yield surface, i.e., if $d\bar{\sigma}\cdot\bar{n} > 0$. Note also that, since $d\bar{e} = d\bar{\varepsilon} - d\bar{\varepsilon}_h$ and $d\bar{e}\cdot\bar{n} = d\bar{\varepsilon}\cdot\bar{n}$, the above expression for $d\bar{S}$ can be rewritten as

$$d\bar{S} = 2G\cdot[d\bar{e} - \frac{2G}{2G+C}\cdot(d\bar{e}\cdot\bar{n})\cdot\bar{n}]$$

But the above equations for the direct and inverse problems are not enough to solve the incremental plasticity problem. As the stresses try to move beyond the yield surface, material hardening effects can cause such surface to translate in stress space and/or change its size and shape. These effects must be computed from hardening rules, as studied in the next sections.

5 KINEMATIC HARDENING

The Bauschinger effect, observed under cyclic loading, is a change in the modulus of the opposite yield strength after strain hardening, due to microscopic stress distribution: tensile cold working up to a stress level $\sigma_x > S_Y$ increases the tensile yield strength in the **x** direction for subsequent loadings from S_Y to σ_x, but it also reduces in absolute value the compressive yield strength, from $-S_Y$ to roughly $(\sigma_x - 2S_Y)$, and vice-versa after a compressive strain hardening. This is a general phenomenon found in most polycrystalline metals, the most significant hardening type after the material becomes cyclically stable.

The Bauschinger effect can be modeled in stress space, allowing the yield surface to translate with no change in its size or shape. In the above example, if the center of the yield surface is translated in the **x** direction of the stress space by $(\sigma_x - S_Y)$, then the resulting surface will intersect the **x** axis in the new tensile yield stress $(\sigma_x - S_Y + S_Y) = \sigma_x$ and in the new compressive yield stress $(\sigma_x - S_Y - S_Y) = (\sigma_x - 2S_Y)$. Since this phenomenon only involves the kinematic translation of the yield surface, it is called *kinematic hardening*.

So, in the deviatoric stress space, kinematic hardening maintains the radius $S_Y\sqrt{6/3}$ of the yield hypersphere fixed, while its center is translated, changing the generalized plastic modulus **C**. Several models can be used to obtain the current value of **C** as the yield surface translates, to calculate the plastic strain increments. One of the most efficient models is the multi-yield-surface model, which uses several yield surfaces obtained from a discretization of the stress-strain curve. The first surface is the one that defines the elastic limit of the material, usually represented in the deviatoric space by a hypersphere with radius $r_1 = S_Y\sqrt{6/3}$, implying that the material is assumed purely elastic for plastic strains below **0.2%** (which define S_Y). Considering n_c surfaces, the values of r_2, r_3, ..., r_{nc} are calculated from the cyclic effective stress-strain curve $\sigma_x\sqrt{6/3}\times\varepsilon_{xp}$, where σ_x and ε_{xp} are obtained from uniaxial tests, see Fig. 2.

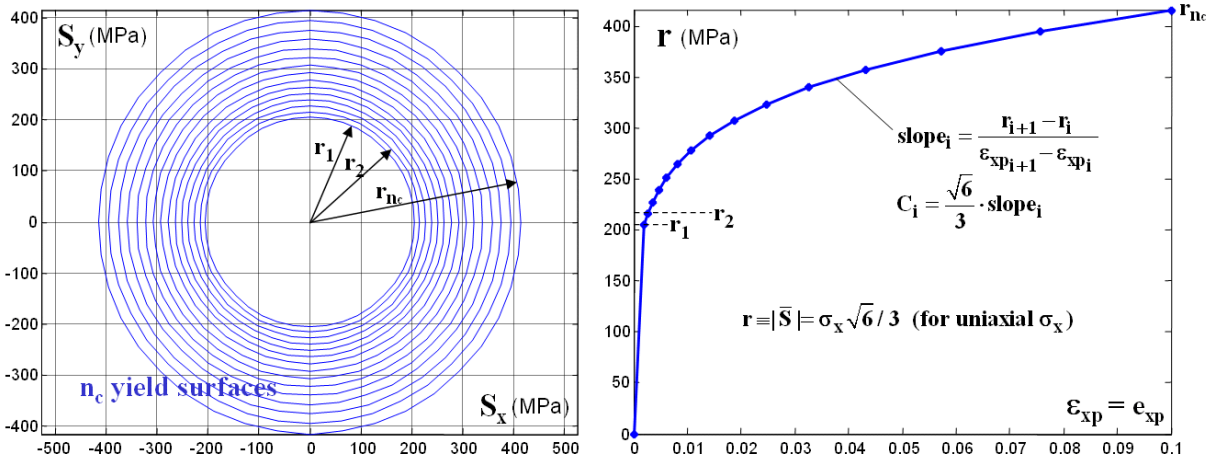

Figure 2. Yield surfaces in the S_x-S_y deviatoric stress space, and correspondent radii obtained from the piecewise linearization of the cyclic effective stress-strain curve.

As seen in the figure, n_c points from the cyclic effective stress-strain curve are chosen to define each of the radii r_i from the yield surfaces, $i = 1, ..., n_c$. The value of the generalized plastic modulus $C = C_i$ between the surfaces with radii r_{i+1} and r_i is

then estimated from the slopes of the cyclic effective curve between points (ε_{xpi}, σ_{xi}) and (ε_{xpi+1}, σ_{xi+1}), by

$$C_i = \frac{2}{3}\cdot\frac{d\sigma_x}{d\varepsilon_{xp}} \cong \frac{2}{3}\cdot\frac{\sigma_{x_{i+1}} - \sigma_{x_i}}{\varepsilon_{x_{pi+1}} - \varepsilon_{x_{pi}}} = \frac{2}{3}\cdot\frac{\sqrt{6}}{2}\cdot\frac{r_{i+1} - r_i}{\varepsilon_{x_{pi+1}} - \varepsilon_{x_{pi}}}, \text{ since } \sigma_x = r\cdot\frac{\sqrt{6}}{2}$$

Note that the difference between the radii of consecutive surfaces is not necessarily the same for all surfaces. To improve the algorithm accuracy, it is a good idea to choose values ε_{xpi} that are logarithmically spaced, resulting in

$$\varepsilon_{x_{p_i}} = \varepsilon_{Yp}\cdot\left(\varepsilon_{fp}/\varepsilon_{Yp}\right)^{(i-1)/(n_c-1)}$$

where ε_{Yp} is a plastic strain below which the material is assumed purely elastic and ε_{fp} is the plastic component of the rupture strain (which is usually approximated by the rupture strain ε_f). The radius of each surface is then calculated by

$$r_i = H_c\cdot\varepsilon_{x_{pi}}^{h_c}\cdot\frac{\sqrt{6}}{3}$$

Note that the usual value $r_1 = S_Y\sqrt{6}/3$ is obtained by making $\varepsilon_{Yp} = 0.2\%$ and $i = 1$. For a better precision, but with a higher computational cost, it is recommended to use a lower value of ε_{Yp} associated with the true elastic limit of the material, usually much smaller than $S_{Y0.2\%}$.

From the above equations, it is possible to obtain all values of r_i and C_i, necessary for the algorithm, described next.

The multi-yield-surface model assumes that the yield surfaces are rings with increasing radii r_i, initially concentric. The rings cannot intersect each other, except when they are tangent. While the vector $\bar{S}$ is moving in the deviatoric space inside the inner ring, with radius r_1, all stress and strain increments are purely elastic. When the vector $\bar{S}$ touches the border of the inner ring, this ring becomes the active surface and starts translating until it touches the next one, which has radius r_2. During this trajectory between r_1 and r_2, the plastic strain increment is calculated using $C = C_1$. The ring r_2 then becomes the active surface.

If the loading is further increased, both rings r_1 and r_2 are translated altogether as a rigid body, until touching the ring r_3. Analogously, during this trajectory between r_2 and r_3, the plastic strain increment is calculated using $C = C_2$. The ring r_3 becomes the active surface and the process continues, until some loading reversal makes the vector $\bar{S}$ move inside the inner ring. During this trajectory inside the inner ring, the strain increments are purely elastic, no surface is active, and therefore none of the rings move. The rings will only move again when $\bar{S}$ touches again the inner ring. Note however that the rings are not concentric anymore. The plastic memory of the material is stored in the model through these positions between centers of the rings.

Figure 3 shows the multi-yield-surface algorithm applied to a 1020 steel under the biaxial loading history [$\sigma_x = \{0 \rightarrow 350 \rightarrow -250 \rightarrow 250\}$MPa, $\sigma_y = -\sigma_x$], with all other stress components equal to zero, for $n_c = 15$ yield surfaces. Note that, in this simple example, the choice of $\sigma_y = -\sigma_x$ and $\sigma_z = 0$ results in $\sigma_h = (\sigma_x + \sigma_y + \sigma_z)/3 = 0$, making $S_x = \sigma_x - \sigma_h = \sigma_x$ and $S_y = \sigma_y - \sigma_h = \sigma_y$.

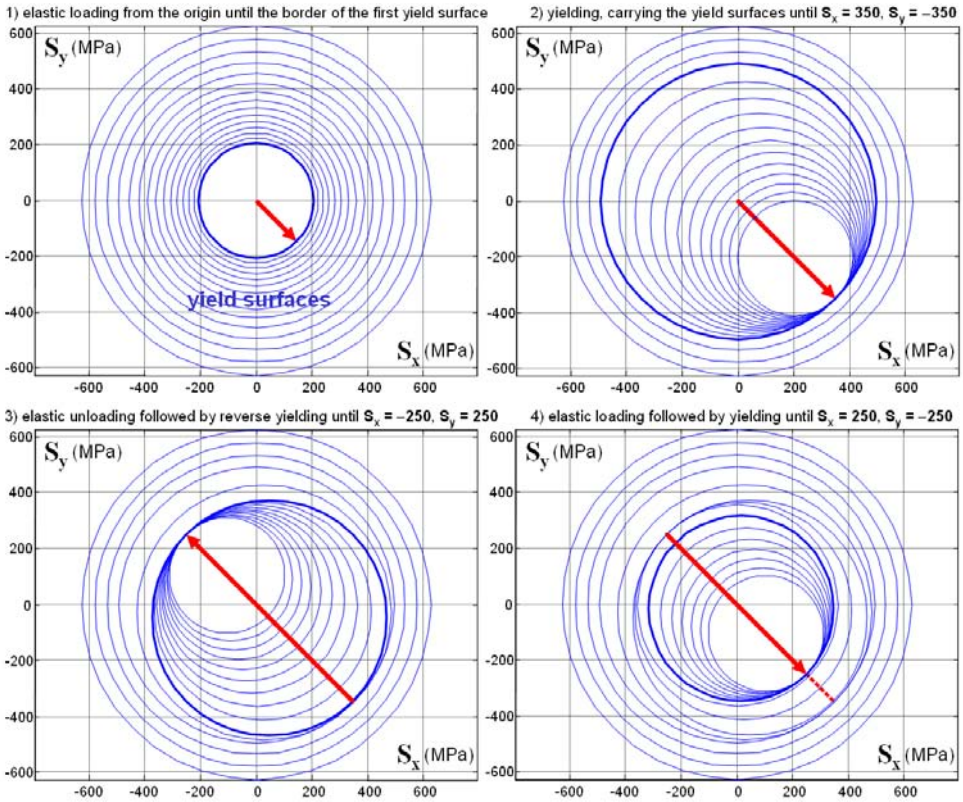

Figure 3. Yield surfaces in the S_x-S_y deviatoric stress space; the active surface (circle) at each loading step is represented with a thicker line.

Under non-proportional loading, the direction along which the deviatoric stress vector $\bar{S}$ moves may be different from the ring translation direction. To calculate the ring translation direction in this general case, two rules have been proposed, one by Mròz[4] and another by Garud.[5]

The Mròz rule[4] assumes that the translation of ring r_i occurs in a direction parallel to the line that joins the current point $\bar{S}$ at ring r_i with the corresponding point $\bar{S}_M$ at the next ring r_{i+1} which has the same normal unit vector $\bar{n}_M$, see Figure 4. In this figure, $\bar{S}_{ci}$ and $\bar{S}_{ci+1}$ are the centers of rings r_i and r_{i+1} in the deviatoric space.

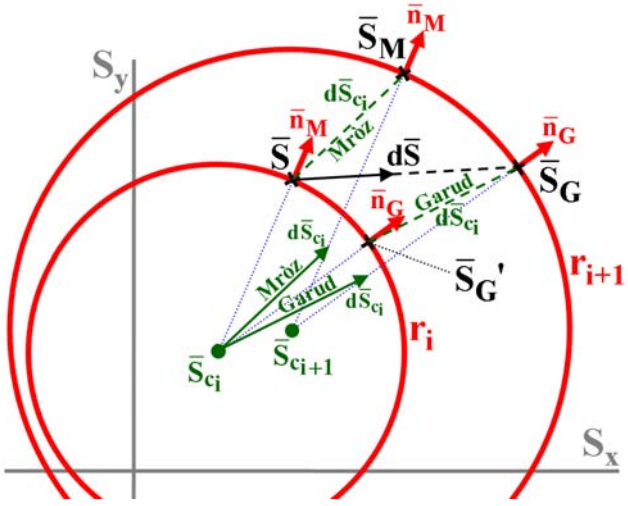

Figure 4. Illustration of Mròz and Garud kinematic hardening rules.

ISSN 1516-392X

However, the Mròz rule can induce a few numerical problems, which can result in rings intersecting in more than one point. Garud's rule[5] does not have such numerical problems, therefore it is our model of choice. It states that the translation of ring $\mathbf{r_i}$ is in a direction parallel to the line that joins the points $\bar{S}'_G$ and $\bar{S}_G$ shown in Fig. 4. The point $\bar{S}_G$ is found from the intersection between ring $\mathbf{r_{i+1}}$ and the vector $\bar{S}+\alpha\cdot d\bar{S}$, where $\alpha > 0$ is a constant that can be determined from such intersection condition. The normal vector $\bar{n}_G$ at $\bar{S}_G$ is then

$$\bar{n}_G = \frac{\bar{S}-\bar{S}_{c_{i+1}}+\alpha\cdot d\bar{S}}{|\bar{S}-\bar{S}_{c_{i+1}}+\alpha\cdot d\bar{S}|}$$

The point $\bar{S}'_G$ is defined as the corresponding point of $\bar{S}_G$ at ring $\mathbf{r_i}$ with same normal unit vector $\bar{n}_G$, see Fig. 4. It is easy to see that the translation vector for the center of ring $\mathbf{r_i}$ is parallel to $d\bar{S}_{c_i}$, where

$$\left.\begin{array}{l}\bar{S}_G = \bar{S}_{c_{i+1}}+\bar{n}_G\cdot r_{i+1}\\ \bar{S}_G{}' = \bar{S}_{c_i}+\bar{n}_G\cdot r_i\end{array}\right\} \Rightarrow d\bar{S}_{c_i} = \bar{S}_G-\bar{S}_G{}' = (\bar{S}_{c_{i+1}}-\bar{S}_{c_i})+\bar{n}_G\cdot(r_{i+1}-r_i)$$

The multi-yield-surface algorithm is summarized in Figs. 5 and 6. Initially, all ring centers $\bar{S}_{c_i}$ are placed at the S_xxS_y plane origin. The ring radii $\mathbf{r_i}$ and the generalized plastic modulii $\mathbf{C_i}$, $\mathbf{i = 1,...,n}$, are calculated from the presented equations. The variable **j** is used to count the loading number from the history, while the variable **i*** stores the number of the currently active ring (if no ring is active, then **i* = 0**).

6 ISOTROPIC HARDENING

Isotropic hardening is characterized by the expansion/contraction of the yield surfaces due to material hardening or softening. In the isotropic cyclic hardening or softening, there is an increase or decrease in material strength due to plastic strain, changing the size or shape of the yield surfaces, an effected partially accounted for by the cyclic $\sigma\times\varepsilon$ curves in the classical (unidimensional) ε**N** theory.
White[6] considered not only the kinematic hardening, which happens due to the translations of the hyperspheres (rings), but also the cyclic hardening (or softening) due to cyclic stresses and strains, which make the unidimensional **h** and **H** Ramberg-Osgood parameters tend to the cyclic $\mathbf{h_c}$ and $\mathbf{H_c}$. Therefore, the transition between the monotonic and cyclic hardening parameters can be modeled.
It has been proposed that isotropic hardening is a function of the applied plastic work $\mathbf{W_p}$, which can be incrementally computed by

$$W_p = \sum dW_p = \sum \bar{\sigma}\cdot d\bar{\varepsilon}_p$$

Assuming the material is pressure-insensitive, thus plastically incompressible, the plastic Poisson coefficient is $\nu_p = 0.5$, and the sum of the plastic normal strain increments must be nil, $d\bar{\varepsilon}_{x_p}+d\bar{\varepsilon}_{y_p}+d\bar{\varepsilon}_{z_p} = 0$. Therefore,

$$\bar{\sigma}_h\cdot d\bar{\varepsilon}_p = \sigma_h\cdot(d\bar{\varepsilon}_{x_p}+d\bar{\varepsilon}_{y_p}+d\bar{\varepsilon}_{z_p}) = 0 \quad \therefore$$

$$dW_p = \bar{\sigma}\cdot d\bar{\varepsilon}_p = (\bar{S}+\bar{\sigma}_h)\cdot d\bar{\varepsilon}_p = \bar{S}\cdot d\bar{e}_p+\bar{\sigma}_h\cdot d\bar{\varepsilon}_p = \bar{S}\cdot d\bar{e}_p$$

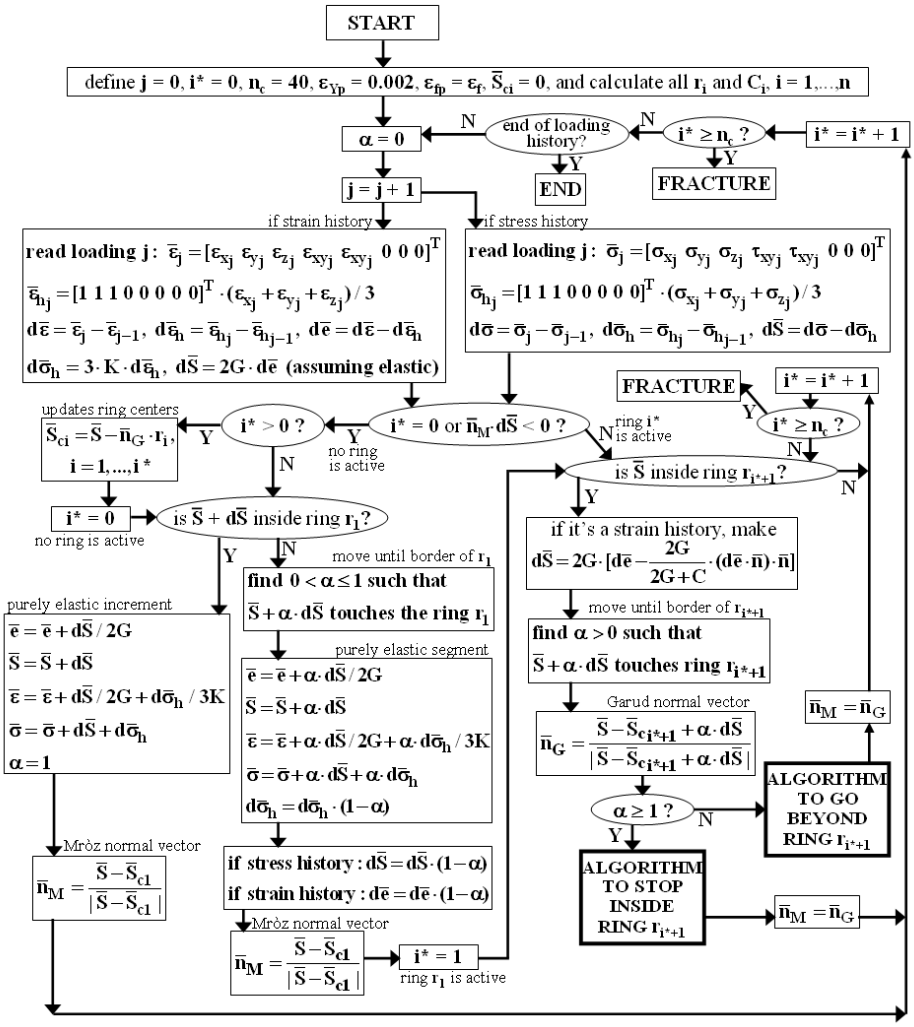

Figure 5. Multi-yield-surface algorithm.

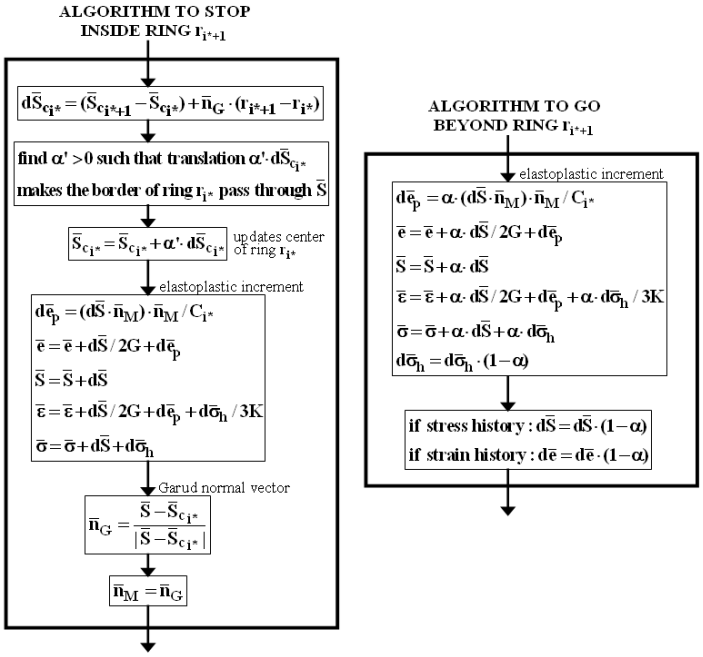

Figure 6. Routines from the multi-yield-surface algorithm to stop inside or to go beyond ring $\mathbf{r_{i^*+1}}$.

So, the plastic work increment can be directly computed from the deviatoric stress and strain tensors. In the multi-yield-surface algorithm, a deviatoric stress increment $\alpha \cdot d\bar{S}$ associated with a plastic deviatoric strain increment $d\bar{e}_p$ from a state $\bar{S}$ results in a plastic work increment

$$dW_p \cong \left[\bar{S} + (\bar{S} + \alpha \cdot d\bar{S})\right] / 2 \cdot d\bar{e}_p = \left(\bar{S} + \alpha \cdot d\bar{S}/2\right) \cdot d\bar{e}_p$$

The above quantity can be easily obtained in the algorithm at every calculation step. Therefore, the accumulated plastic work can be calculated.
Cyclic hardening can then be empirically considered in the multi-yield-surface algorithm through the expressions for the transient hardening coefficient H_t and exponent h_t

$$H_t = H_c + \frac{H - H_c}{1 + (\sum dW_p)^{h^*}} \quad \text{and} \quad h_t = h_c + \frac{h - h_c}{1 + (\sum dW_p)^{h^*}}$$

where **h*** is a material-dependent adjustable exponent.

7 CONCLUSIONS

The proposed incremental plasticity algorithm is computationally efficient, calculating the hysteresis loops faster than traditional implementations. It is entirely formulated on the deviatoric stress-strain space, resulting in much simpler equations for the stress or strain increments. The algorithm can capture phenomena such as ratcheting, cyclic hardening or softening, and non-proportional hardening. Damage models that incorporate both strain and stress effects can then be applied.

REFERENCES

1 SOCIE, D.F.; MARQUIS, G.B.. Multiaxial Fatigue, SAE 1999.
2 MEGGIOLARO, M.A.; CASTRO, J.T.P. Comparação entre métodos de previsão de vida à fadiga sob cargas multiaxiais I: modelos tensão-vida e deformação-vida", Anais do 60º Congresso Anual da ABM, p.1976-1985, 2005.
3 MEGGIOLARO, M.A.; CASTRO, J.T.P. Comparação entre métodos de previsão de vida à fadiga sob cargas multiaxiais II: relações tensão-deformação, Anais do 60º Congresso Anual da ABM, p.1986-1995, 2005.
4 MRÒZ, Z. On the description of anisotropic work hardening. Journal of Mechanics and Physics of Solids, v. 15, n. 163, p. 175, 1967.
5 GARUD, Y.S. A new approach to the evaluation of fatigue under multiaxial loadings. Transactions of the ASME, Journal of Engineering Materials and Technology, v. 103, p. 118-125, 1981.
6 WHITE, C.S., A Two Surface Plasticity Model With Bounding Surface Softening , Journal of Engineering Materials and Technology, v. 118, n. 1, p. 37-42, 1996.